Technical Report of Resilient Subpath-Based NDN Transport Protocol for Ad-Hoc Stationary Wireless Sensor Networks

Boyang Zhou
Zhejiang Lab
zhouby@zhejianglab.com

Abstract

Reliable data transport in ad-hoc stationary wireless sensor networks (WSNs) powered by sustainable energy sources is challenging due to packet losses caused by noise interference. Traditional transport protocols often neglect the role of subpaths—available routes between nodes and the sink—which are critical for enhancing resiliency. To address this, we propose RNTP, a subpath-based transport protocol leveraging named-data networking (NDN) to improve packet delivery reliability and efficiency. RNTP constructs subpaths with minimal overhead, dynamically selecting reliable routes based on channel quality and hop distance. It incorporates congestion control and fast retransmission mechanisms to optimize end-to-end performance. Simulations demonstrate that RNTP outperforms existing protocols in terms of delivery reliability, latency, and energy efficiency across various network conditions.

1 Introduction

Ad-hoc stationary wireless sensor networks (WSNs) play a critical role in IoT applications such as environmental monitoring, industrial automation, smart grids, and healthcare systems [1, 2, 3]. These networks, often powered by sustainable energy sources like solar panels, require reliable data transport to ensure continuous and accurate monitoring [4]. However, packet losses caused by wireless noise, interference, and congestion pose significant challenges to reliable data delivery [3].

Traditional transport protocols primarily rely on end-to-end paths, which can suffer from failures due to unpredictable channel conditions [5, 6, 7]. Subpaths, defined as partial routes between intermediate nodes and the sink, offer greater resilience by enabling dynamic rerouting and congestion avoidance. However, existing approaches fail to fully leverage subpaths, often leading to inefficiencies in packet delivery and increased energy consumption [8, 9, 10].

To address these challenges, we propose RNTP, a resilient subpath-based transport protocol leveraging Named-Data Networking (NDN) [11, 12, 13]. The source code of resilient subpath-based NDN transport protocol (RNTP) has been released online (https://github.com/zhouby-zjl/rntp). RNTP constructs subpaths with minimal overhead using a single reactive message propagation process. At each hop, it dynamically selects the most reliable subpath based on channel quality (CQ), considering both hop distance and signal-to-interference-plus-noise ratio (SINR) [14]. It integrates feedback-driven congestion control and fast retransmission mechanisms to improve end-to-end packet delivery and energy efficiency.

Our simulations in ndnSIM demonstrate that RNTP significantly reduces packet loss, delivery time, and energy consumption compared to existing approaches. In a 64-node topology under noise interference, RNTP achieves a 0.02% end-to-end failure rate (EEFR) and a 5.54s end-to-end delivery time

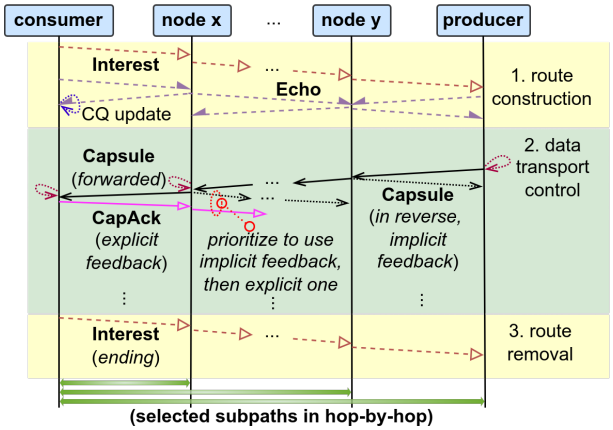

Figure 1: Overall interactions of RNTP

(EEDT), outperforming conventional protocols [15, 16]. Furthermore, experiments across WSNs with 36 to 144 nodes confirm RNTP's scalability and robustness in dynamic, resource-constrained environments.

2 Protocol

Building on the consumer-driven model of NDN, the proposed RNTP enhances resilience and efficiency in ad-hoc stationary WSNs by introducing *subpaths* and a robust transport mechanism.

Fig. 1 illustrates RNTP's interactions. A consumer requests payloads from a producer, and data is transmitted hop-by-hop along selected subpaths. Four NDN-compatible type-length-value (TLV) messages—*Interest*, *Echo*, *Capsule*, and *CapAck*—facilitate routing and transport [17].

RNTP ensures *resilient and efficient transport* through two key mechanisms:

2.1 Subpath Routing

RNTP enables *localized* routing by maintaining *partial paths*, which collectively form end-to-end routes. Unlike address-based approaches, RNTP embeds subpath information in messages, enabling *adaptive routing* [11].

Subpaths are categorized as:

- **Trunk subpath:** Primary route from consumer to an intermediate hop.
- **Branch subpaths:** Disjoint alternative routes from a trunk node to the producer.

Fig. 2 shows an example in an IEEE 802.11a network, where node **64** has a trunk subpath (1, 10, 19, 21, 31, 48, 64) and branch subpaths (48, 56, 64) and (48, 63, 62, 64). Disjoint branches ensure *interference-free transmission*.

RNTP prevents loops using a *path vector approach*, where *Interests* embed visited nodes. Nodes periodically send *Echos* to update channel quality (CQ) metrics, ensuring optimal subpath selection. Route expiration is managed via *ending Interests* sent by the consumer.

2.2 Subpath-Based Data Transport Control

RNTP employs *hop-by-hop transport control* using implicit and explicit feedback:

- **Implicit feedback:** Downstream nodes confirm reception via wireless broadcasting, reducing overhead.

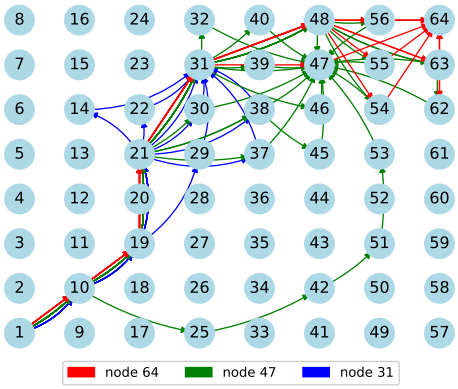

Figure 2: Example of subpath routes at various nodes in simulation [18]

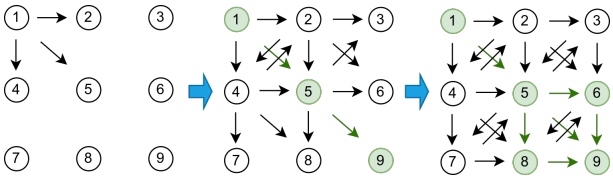

Figure 3: Subpath route construction process

- **Explicit feedback:** *CapAck* messages confirm delivery and detect duplicates.

These feedback mechanisms support:

- **Congestion control:** Nodes adjust forwarding rates based on traffic conditions.
- **Fast retransmission:** Lost packets are recovered via *alternative branch subpaths*, enhancing reliability.

By integrating *subpath routing* with *localized transport control*, RNTP enables *efficient and resilient data transport* in lossy and dynamic WSNs. The following sections detail its performance and implementation.

2.3 Subpath-Based Routing

To address challenge 1, RNTP integrates named-data network (NDN)'s Interest-based retrieval with subpath routing, leveraging CQ values for efficient selection.

2.3.1 Efficient Route Management

RNTP constructs subpath routes using NDN's Interest propagation:

- Each node broadcasts only the first received Interest to avoid loops.
- Interest trajectories are recorded with CQ metrics (e.g., signal-to-interference-plus-noise ratio (SINR)).

Fig. 3 illustrates subpath formation in a 9-node grid. The constructed paths include a trunk subpath (1, 5) and branch subpaths (5, 9), (5, 6, 9), and (5, 8, 9).

Efficiency: Each node forwards an Interest once, reducing overhead to $O(n)$. Path length scales as $O(\max(u, v))$ in a $u \times v$ grid and $O(n)$ in linear topologies. Routes are removed via an ending Interest, ensuring minimal overhead.

2.3.2 Route Table and CQ Measurement

Each node maintains a route table $\Upsilon = \{(\rho, \Omega_\rho)\}$, where ρ is a subpath, and Ω_ρ stores CQ values. The CQ metric (ω_b^j) is updated within a bounded time using:

$$\omega_b^j = \begin{cases} \alpha\omega_b^j + (1-\alpha)\text{SINR} & \text{if arrival} \wedge \omega_b^j \neq \text{broken} \\ \text{SINR} & \text{if arrival} \wedge \omega_b^j = \text{broken} \\ \text{broken} & \text{if no arrival} \end{cases} \tag{1}$$

$$PIAT_{\text{est}} = \min\left(-\frac{\log(1-\theta_{\text{piat}})}{\lambda_{\text{mean}}}, \text{PIAT}_{\max}\right) \tag{2}$$

2.3.3 Optimized Subpath Selection

RNTP selects high-metric subpaths for reliable Capsule forwarding based on:

- *Hops:* Fewer hops reduce latency.
- *SINRs:* Higher SINRs improve reliability.

The subpath metric is computed as:

$$\text{metric}(\Omega_\rho) = \left(\prod_{2 \leq u \leq b} \omega_u\right)^{1/(2\cdot(b-1))} \tag{3}$$

To ensure robustness, LookupSubpath($\Upsilon, k, \rho_{\text{prev}}$) selects candidate subpaths avoiding broken CQ values and overlapping with upstream nodes of ρ_{prev}:

$$P' = \{(\rho', \text{metric}(\Omega'_\rho)) \mid (\rho', \Omega'_\rho) \in \Upsilon \wedge \text{broken} \notin \Omega'_\rho \wedge \rho' \cap U = \emptyset\} \tag{4}$$

If P' is non-empty, the k'-th highest metric subpath is chosen ($k' = k \mod |P'|$), ensuring diverse subpath utilization and reducing congestion. This approach enables adaptive, high-quality subpath selection for resilient data transport.

2.4 Resilient Subpath-Based Data Transport Control

RNTP builds on the selected high-metric subpaths to enable a robust hop-by-hop transport control mechanism. This integrates path-vector-based Capsule forwarding, adaptive congestion window (CWnd) adjustment, and fast retransmissions, supported by a FIFO-based content storage (CS) for efficient retransmission. Unlike conventional approaches prone to excessive retransmissions and congestion in stationary wireless sensor networks (WSNs), RNTP mitigates end-to-end packet delivery failure rate (EEFR) and end-to-end packet delivery time (EEDT), ensuring reliable Capsule delivery under dynamic and lossy conditions.

2.4.1 Robust Subpath-Based Capsule Forwarding

Path-vector-embedded Capsules enhance payload delivery by improving both reliability and efficiency. Each node processes incoming Capsules based on two rules:

- If the path vector is non-empty and the next-hop CQ meets a threshold, the Capsule follows the vector.

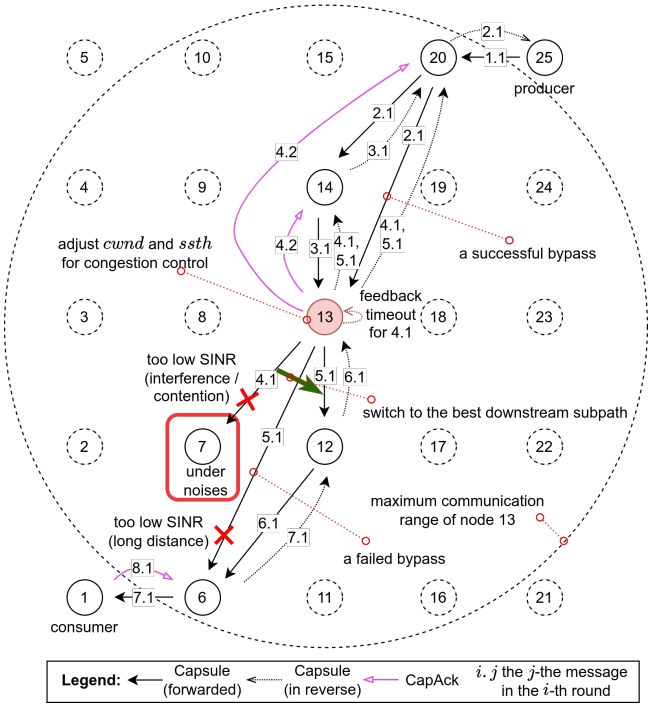

Figure 4: Capsule transport process: solid circles denote route nodes, dashed circles denote others. Labels "i, j" indicate round and sequence numbers.

- Otherwise, a locally selected high-quality subpath replaces the downstream portion.

This enables two key features:

- *Efficient subpath failover*: Nodes dynamically select alternative subpaths upon failure. For instance, if node 13 detects a failure to node 7, it retrieves the Capsule from CS and reroutes via subpath 2 (12, 6, 1), ensuring uninterrupted transport.
- *Immediate node bypass*: Capsules opportunistically bypass intermediate nodes, reducing latency and hop count. For example, Capsule 2.1 from node 20 bypasses node 14 to reach node 13, provided sufficient SINR.

By combining these features, RNTP significantly improves resilience and efficiency in ad-hoc stationary WSNs.

2.4.2 Resilient Transport Control

Building on subpath-based forwarding, RNTP employs a transport control policy leveraging implicit and explicit feedback to ensure reliable and efficient data delivery.

- *Implicit feedback (Capsule in downstream):* The successful forwarding of a Capsule implicitly confirms its reception upstream, reducing message overhead. For example, node 13 accepts Capsule 2.1 from node 20 and forwards Capsule 4.1, signaling successful delivery to upstream nodes.
- *Explicit feedback (CapAck in downstream):* Upon receiving a Capsule, the consumer or intermediate nodes send a CapAck to upstream nodes, preventing redundant retransmissions.

This policy optimizes transport via:

(i) Congestion control. Each node adjusts its CWnd (*cwnd*) using additive increase and multiplicative decrease (AIMD), balancing efficient utilization and congestion avoidance:

Table 1: Congestion control policy in RNTP

Event	Next Hop	Congestion Window Size ($cwnd$)	Slow Start Threshold ($ssth$)
Feedback received	Available	$\begin{cases} 2 \times cwnd, & 1 \leq cwnd < ssth \\ cwnd + 1, & cwnd \geq ssth \end{cases}$	$ssth + 1$
Feedback timeout	Broken	0	$\max(ssth/2, 1)$
	Available	$\max(cwnd/2, 1)$	
Any RNTP message arrival	Available	$cwnd_{\text{init}}$, if $cwnd = 0$	$ssth_{\text{init}}$, if $cwnd = 0$
Transport initialization	Available	$cwnd_{\text{init}}$	$ssth_{\text{init}}$

- When next hops are available, $cwnd$ increases—doubling in slow start ($1 \leq cwnd < ssth$) and incrementing linearly in congestion avoidance ($cwnd \geq ssth$).
- When next hops fail, $cwnd$ is halved until zero, preventing congestion.
- Upon restoration or initialization, $cwnd$ and $ssth$ reset to configurable initial values.

Table 1 details these rules.

(ii) Retransmission. Each Capsule can be retransmitted up to $\eta_{\max}$ times until valid feedback is received. Retransmission occurs upon a timeout (τ_{cap}) and proceeds along a high-metric subpath if available; otherwise, it is paused to avoid congestion.

Since retransmissions may cause out-of-order arrivals, the consumer temporarily buffers Capsules and triggers resequencing after a predefined timeout, ensuring in-order delivery to the application layer.

These mechanisms collectively enhance RNTP's resilience and efficiency under dynamic network conditions (see Section 3.3).

Summary RNTP integrates subpath routing and hop-by-hop transport control to address challenges in NDN-based ad-hoc stationary WSNs. By leveraging NDN's name-based routing and in-network caching, it ensures reliable and efficient data transport in challenging environments.

3 Performance Evaluation

The performance of RNTP was comprehensively evaluated with comparisons within challenged ad-hoc stationary WSNs.

3.1 Simulation Environment

The simulation environment was realized to reproduce the data transport process of ad-hoc stationary WSNs using various schemes. The key components are detailed as follows.

(i) **Network simulation**. We conducted simulations using ndnSIM [15] to model a stationary ad-hoc WSN compliant with the IEEE 802.11a standard [19] with a high density. WSN consists of 64 nodes in an 8×8 grid, with 20-meter spacing between nodes. Transmission power and receive gain are 16.02 dBm and 0 dB. Channels use light signal speed and the log-distance propagation loss model [20], operating at an orthogonal frequency division multiplexing rate of 6 Mbps adjusted by the classical adaptive auto rate fallback algorithm [21]. Each message reached an average of 14.5 neighbors, with the maximum of 20, indicating high connectivity density.

We tested route scalability with 16, 36, 64, 100, and 144-node grid topologies. This configuration is suitable for testing.

(ii) **Data transport schemes**. Within the established WSN, data transport simulation involves transmitting 1000-byte payload packets from a source node to a sink node upto 10 pps, a rate chosen for

stressing the network's channel capacity. Various data transport schemes were evaluated in this study for comprehensive performance comparison as follows.

Classical data transport protocols TCP [22] and UDP [23] were evaluated in combination with widely used routing protocols ad hoc on-demand distance vector routing (AODV) [5], dynamic source routing (DSR) [6], and destination-sequenced distance-vector routing (DSDV) [24], employing their default configurations as specified in the literature to ensure reproducible baselines. Minor adjustments were applied to the default configurations of these protocols for the WSNs:

- *TCP:* Nagle algorithm disabled for timeliness; segment size set to 1000 B to match the payload; retry limit set to 3 ($\eta_{\max}$); 2 MB buffer to prevent overflow.
- *UDP:* Standard configurations retained, as UDP does not include reliability features.

Advanced data transport protocols, including data-centric ad-hoc forwarding (DAF) [12], cache-aware congestion control mechanism (RT-CaCC) [8], and fast rerouting protocol (FRP) [7], were implemented according to their respective papers. DAF uses default parameters ($\alpha = 7/8$, $\beta = 3/4$), while RT-CaCC and FRP require no parameter adjustments, ensuring fair and accurate comparisons.

Additionally, the source code of our RNTP is publicly available on GitHub [18], with the following key parameters:

- $\alpha = 0.1$ for SINR fluctuation management.
- $\nu_{\max} = 3$ to establish subpaths in collisions.
- $w_{\max} = 50$ ms to reduce Interest signal collisions.
- $\eta_{\max} = 3$ for reliable retransmissions.
- $\tau_{\text{cap}} = 0.1$ s as the maximum round-trip time.
- $cwnd_{\text{init}} = 64$ packets, leveraging bandwidth per hop.
- $ssth_{\text{init}} = 128$ packets, double $cwnd_{\text{init}}$, for congestion window growth.
- $\tau_{\text{echo}} = 1$ s for failure detection.
- $\theta_{\text{piat}} = 99.9999\%$ for precise PIAT estimation.
- $\tau_{\text{piat}} = 3.1$ s (calculated as $3 \times \tau_{\text{echo}} + \tau_{\text{cap}}$) for channel failure detection.

These parameters were selected to balance reliability and efficiency, based on extensive testing across different network conditions (described later). Standardized settings of the these schemes ensure reproducibility and unbiased comparison.

(iii) **Simulation of channel failures**. We simulated wireless NIC channel failures by introducing noise levels distributed in a Gaussian pattern across a specific number of node failures (NN) randomly selected. Noise ranged from 0 to 30 dB with a variance of 5 dB, causing varying levels of packet loss, potentially leading to complete channel failure. When a NIC failed, it affected all interactions with other nodes.

Each test case started data transmission at 0 s, with node failures between 5 s and 15 s, and the source ceased sending payload packets at 20 s. This sequencing included periods of normal operation, failure, and recovery, to fully support tests.

(iv) **Simulation with solar renewable energy sources**. To analyze the performance of RNTP under realistic conditions, we conducted hybrid simulations that combined ndnSIM for network-level

metric evaluation and pvlib [25], a photovoltaic simulator, for solar renewable energy input modeling. This setup provided a comprehensive understanding of RNTP's behavior in terms of both network and energy performance.

Each WSN node operated with RNTP and was powered by a battery with a usable capacity of 15 000 mAh, continuously charged by a 40 W Siemens solar module ST40 [26]. This configuration reflects real-world outdoor WSN deployments [27, 28]. Solar panel performance was simulated using pvlib, based on Sandia's photovoltaic array performance model [29].

The simulations utilized real weather data from Hangzhou, China (latitude 30.25°, longitude 120.16°), collected between 2008 and 2017 by the European Commission [30]. The dataset included hourly temperature, solar irradiance, and solar position relative to the location. Simulations spanned a 10-year period, using daily and seasonal variations in solar energy availability from each year to ensure the results reflected long-term energy sustainability for outdoor WSN deployments.

3.2 Experiment Cases and Metrics

Within the above stationary WSN environment with protocol configurations under channel failures, the performance of RNTP was comprehensively evaluated on three key aspects:

(i) **Assessing the performance of RNTP**. This evaluation tested RNTP under varying noise interference levels and NN in the WSNs, focusing on the following cases and metrics:

- *Data transport capabilities.* Metrics tested include EEFR, EEDT before resequence (EEDT-N), EEDT after resequence (EEDT-R) (under 0% out-of-order rate (OOR)), Capsule sending queue size, and message costs. EEDT for lost payload packets was set to 60 s as an upper bound, while EEDT for successfully transmitted packets reflected actual conditions. The CapAck ratio is defined as the number of CapAck messages sent per Capsule, serving as an indicator of feedback efficiency.

- *Congestion control responsiveness.* To test this, we select a pair and expose NN of 15 to 30 dB noise interference, to observe how CWnd adapts to various events. This scenario facilitated the observation of subpath variations at the consumer, assessed through two metrics: (a) subpath similarity ratio (SSR), indicating the ratio of current in-path node identifiers (IDs) to the length of the highest-metric path; and (b) fault overlapping ratio (FOR), representing the proportion of faulty channels in the current path.

- *Subpath route scalability.* To examine that, we tested route quality at each hop across various network scales using two measurements: the highest-metric subpath, and reroute stretches in metric and subpath length. The stretch is the difference between the highest-metric subpath and rerouted subpaths at each hop, revealing rerouting cost.

(ii) **Testing energy consumption of RNTP**. Energy evaluation was conducted under the two key conditions:

- *Network loads*: Producer's Capsule sending frequency (PSF) from 4 to 10 pps, simulating light to heavy traffic.

- *Channel failures*: Various noises added to NN channels as described earlier, simulating realistic wireless challenges.

The key energy metrics evaluated are listed below:

- *Effective energy consumption (EEC)*: Energy consumption per successfully received payload packet, in J, capturing the balance between energy usage and transport success.

- *Energy consumption rate (ECR)*: The energy consumption rate, measured in watts, indicating the average energy consumed per second during transmission. This metric provides insight into per-node energy dynamics.

- *Remaining battery energy (RBE)*: Residual battery energy, expressed in mAh, indicating remaining capacity. It analyzes the long-term sustainability of the network.

(iii) **Comparing performance**. Fair comparisons between RNTP and other schemes were performed in the 64-node topology under varying noise levels. Essential metrics included EEFR, EEDT (excluding TCP without resequence), and EEC.

EEC's selection rationality for energy comparisons. Excluding ECR and RBE as discussed earlier, EEC was chosen as the most relevant energy metric for cross-protocol comparisons. This is because EEC reflects the actual energy efficiency of successfully delivered packets, accounting for signaling overhead and the effectiveness of transport protocols. In contrast, the other two metrics have the following drawbacks:

- The ECR can be influenced by biases introduced by varying EEFRs, which impact overall energy consumption, as demonstrated in Section 3.4. Evaluated by ECR, protocols with high EEFR often appear energy-efficient, as their transport processes are frequently suspended to recover lost payload packets. Differently, RNTP achieves significantly lower EEFR by sustaining active transport processes, incurring slightly higher ECR. This can lead to a false sense of efficiency while compromising reliability.

- The RBE does not account for discrepancies in payload delivery success, which makes it less reliable for fair evaluation of transport performance across protocols. Similar to ECR, RNTP can achieve a higher RBE, but RBE alone does not reflect delivery success, which is crucial for evaluating transport efficiency.

Hence, EEC provides a fair and consistent comparison by quantifying the energy cost per successfully delivered packet, directly linking energy consumption to delivery performance.

3.3 Performance of RNTP

3.3.1 Data Transport

Fig. 5 illustrates variations in different performance metrics under various noise interference levels corresponding to NNs of 5, 10, and 15. These figures are complemented with their mean and 95th percentile performance statistics summarized in Table 2. Together, they highlight RNTP's exceptional performance, which is discussed below.

(i) **High reliability**. As shown in Fig. 5(a), EEFR remains at 0% for NN cases when noise means do not exceed 15 dB. At higher noise means, EEFR shows minimal occurrences, with maximum values reaching only 1% under serious interference.

The occasional loss of Capsules can be attributed to transient loops among divergent subpaths at the current node, causing a forwarding deadlock at downstream nodes, as illustrated in Fig. 6. For instance, consider ρ_1 (A, B, C, E, H) and ρ_2 (B, D, E, C, G). If Node B tries to send Capsule M_4 via ρ_1, it may fail to receive a feedback within $\eta_{\max}$ despite reaching node C. Node B then switches to ρ_2 and retries sending the Capsule. However, when the Capsule reaches node C via ρ_2, node C drops it because it has already been successfully forwarded to node E. Similarly, when the Capsule reaches node E via ρ_1, Node E drops it as it has already been received by node C. This sequence halts the delivery of the Capsule. Although transient loops are rare, they can occur. Nonetheless, RNTP significantly enhances performance (see Section 3.5).

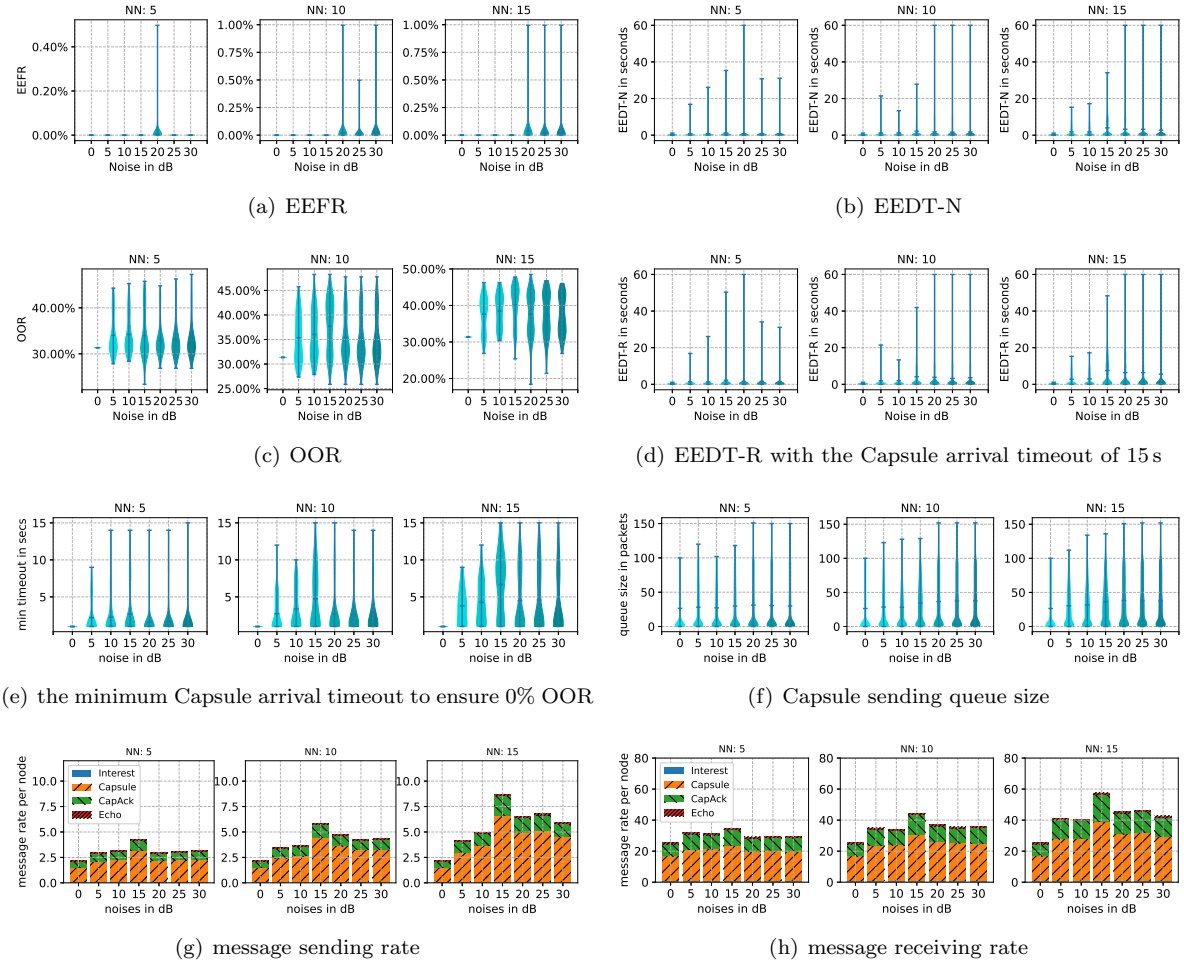

(a) EEFR

(b) EEDT-N

(c) OOR

(d) EEDT-R with the Capsule arrival timeout of 15 s

(e) the minimum Capsule arrival timeout to ensure 0% OOR

(f) Capsule sending queue size

(g) message sending rate

(h) message receiving rate

Figure 5: Performance of RNTP under various levels of noise interference for different NNs in the 64-node WSN

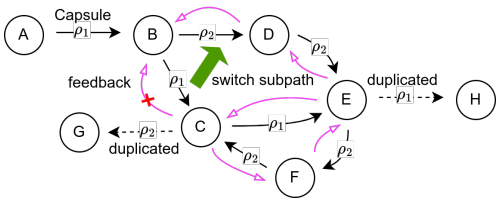

Figure 6: Capsule losses caused by transient states during a subpath failover

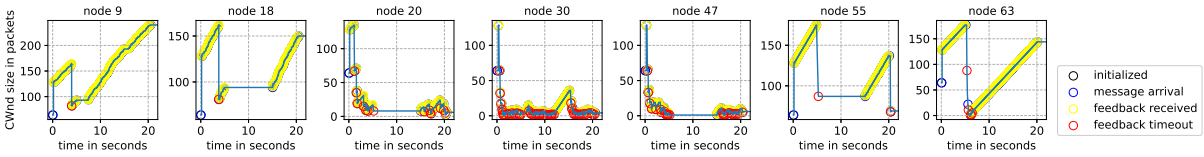

Figure 7: Congestion window changes of RNTP during data transport from node 63 to node 0 in the 64-node WSN under 30 dB noise interference for 15 NN

(ii) **Low delay under noises**. As illustrated in Fig. 5(b), EEDT-N increases with higher noise means. Higher noise levels can lead to channel failures in nodes, triggering subpath failovers. The failover temporarily restricts Capsule sending in the queue, increasing EEDT-Ns. However, EEDT-Ns are still significantly less than comparative schemes (see Section 3.5).

(iii) **Out-of-order Capsules and resequence**. Variations in EEDT-N depicted in Fig. 5(c) result in occasional out-of-order occurrences due to Capsule bypassing and subpath failovers. These are effectively managed by the consumer's resequencing with an arrival timeout of 15 s, as demonstrated in Fig. 5(d), achieving 0% OOR while slightly increasing EEDT-R. Nevertheless, EEDT-R remains much lower compared to existing schemes (see Section 3.5). Fig. 5(e) illustrates the minimum arrival timeout required to achieve 0% OOR, validating our experimental choice of 15 s for consistency. Fig. 5(f) shows the queue sizes variations, with the maximum size of 150 p. These statistics indicate the resequence effectiveness.

(iv) **Efficiency message exchange**. Figs. 5(g) and 5(h) demonstrate the average message rate per second at each node measured for different message types. The CapAck ratio (shown in Table 2) ranges from 29.28% to 43.26% across all test cases, reflecting the use of implicit feedback in RNTP. Additionally, the average number of Interest sending per node is 2.97 p that approximates to $\nu_{\max}$, indicating a subpath route complexity of $O(n)$. The number of received packets is magnified due to the network high density. These statistics underscore the message efficiency of RNTP.

The above statistics consistently affirm RNTP's efficiency.

3.3.2 Congestion Control

Figs. 7 and 8 show the congestion control process and subpath changes of a pair, where the highest-metric path is (0, 9, 18, 20, 30, 47, 55, 63). Between 5 to 15 s, 15 nodes experience 30 dB noise interference. Notably, nodes 18, 20, 47, and 55, which overlap with failure nodes, lie on the path. Fig. 7 depicts changes in CWnd annotated with corresponding events. Fig. 8 presents SSR and FOR for each arriving Capsule at the consumer over time.

During the period from 5 s to 15 s, SSR experiences fluctuations and decreases to 50%, indicating subpath adjustments to avoid channel failures. Concurrently, FOR fluctuates and eventually drops to 0%, signifying successful failover events. At the onset of the failure period, nodes 18, 20, 47, and 55 – overlapping with failure nodes – see their CWnds halve and remain unchanged until the period ends (see Fig. 7), as Capsule delivery switches to an alternative subpath involving nodes 9, 30, and 63, each exhibiting changes in CWnd. This underscores the efficacy of the congestion control process.

3.3.3 Subpath Route Scalability

Fig. 9(a) displays a boxplot illustrating the number of subpaths per node across different topology scales. The mean and maximum values are constrained to 13.94 and 20, respectively, both of which are less than the maximum 20 neighbors, regardless of the increase in n. This observation supports a complexity of $O(\#\text{neighbors})$, simplified to $O(1)$, as discussed in Section 2.3.

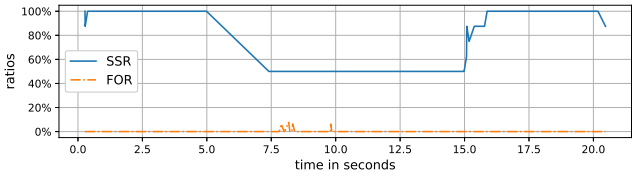

Figure 8: Corresponding subpath changes of RNTP observed at the consumer

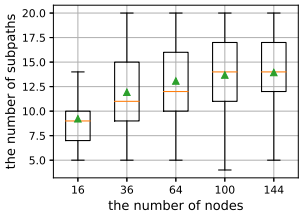

(a) the number of subpaths

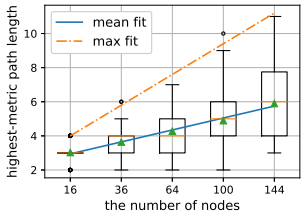

(b) the highest-metric path length

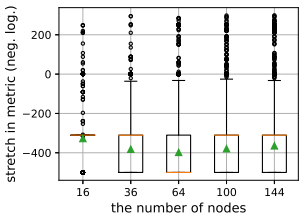

(c) reroute stretch in metric

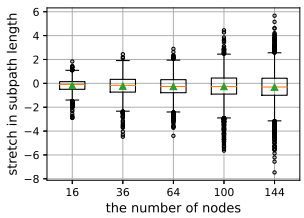

(d) reroute stretch in subpath length

Figure 9: Subpath route quality of RNTP in the 16 to 144-node WSNs

Furthermore, Fig. 9(b) shows that the mean and maximum path lengths adhere to $O(0.35 \cdot n^{1/2} + 1.55)$ and $O(0.9 \cdot n^{1/2} + 0.4)$, respectively, affirming the scalability of routes.

Moreover, reroute stretches were assessed for quality across the topology scales. Fig. 9(c) shows the stretch in metric on a negative logarithmic scale, where the lowest 0 stretch is represented as -500. Fig. 9(d) shows the stretch in subpath length. Both show increased diversity with the scales due to varied subpath trajectories, but RNTP prioritizes high-metric subpaths. Despite that, the average metric stretch remains extremely low ($10^{-398.01}$ to $10^{-327.51}$). Meanwhile, the mean length stretch slightly decreases from -0.18 to -0.32. These statistics consistently indicate favorable stretches of rerouted subpaths, highlighting the efficacy of the rerouting strategy.

3.4 Energy Consumption of RNTP

EEC and ECR. Fig. 10(a) shows the relationship between the energy consumption of RNTP and its message exchange performance in the 64-node topology. The data presented include the average EEC (left y-axis) and ECR (first y-axis on the right), as well as the corresponding message sending rate per node (second y-axis on the right) and average EEFR (third y-axis on the right). The tests were under varying PSFs of 4, 6, 8, and 10 pps, with channel failures characterized by NNs from 0 to 30 and mean noise levels from 0 to 40 dB.

Under all conditions, EEC and ECR exhibit minimal variations for the respective PSFs. EEC remains below $1.73 \cdot 10^{-4}$, $3.86 \cdot 10^{-4}$, $7.13 \cdot 10^{-4}$, and $1.24 \cdot 10^{-3}$, while ECR is limited to $8.66 \cdot 10^{-4}$, $1.53 \cdot 10^{-3}$, $3.56 \cdot 10^{-3}$, and $6.22 \cdot 10^{-3}$. This stability reflects the consistent message rates, which remain below 0.61, 0.93, 2.21, and 4.14 pps, respectively, as energy consumption is primarily driven by message transmissions.

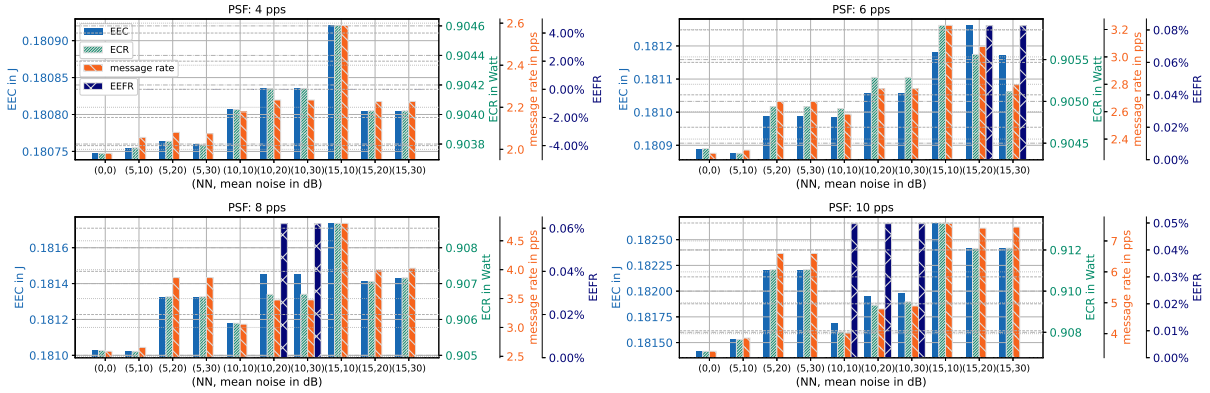

(a) average EEC, ECR, and message sending rate per node, with each tick on the x axis in the format (NN, mean noise in dB)

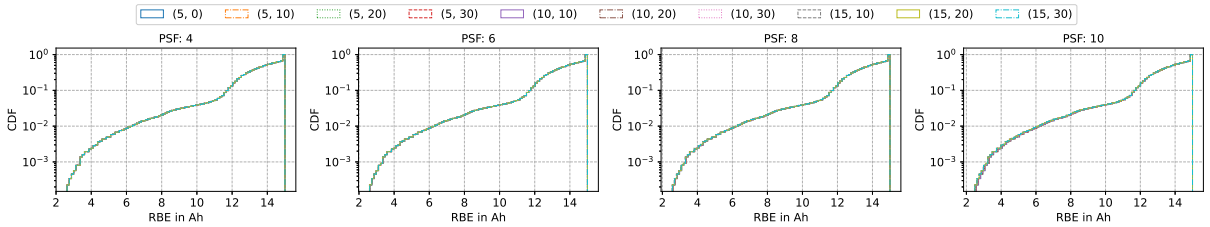

(b) CDF of RBE across all nodes, with each legend label in the format (NN, mean noise in dB)

Figure 10: Energy performance of RNTP in a 64-node WSN under varying network loads (PSF) and conditions (NNs and noise interference levels)

Anomalies are observed when NN reaches 15 with a mean noise level of 10 dB. In the conditions, peak values of EEC and ECR are observed, corresponding to an increased message rate. This behavior underscores the adaptability of RNTP's congestion control mechanism, which dynamically adjusts message rates to manage Capsule losses while ensuring network stability. Such adaptability shows RNTP's ability to keep energy efficiency even under challenging network conditions.

Furthermore, the variations in EEC closely mirror those in ECR, exhibiting a nearly linear relationship when the mean EEFR is close to zero. The energy consumed for retransmitting lost Capsules offsets the energy used for successful deliveries, causing an increase in EEC. In contrast, scenarios with 0% mean EEFR demonstrate a proportional relationship between EEC and ECR, reflecting both the rate and total energy consumption. These findings suggest ECR is a more appropriate metric for cross-protocol comparisons, as it offers a clearer measure of energy efficiency independent of delivery success.

RBE. Fig. 10(b) illustrates the CDF of RBEs (logarithmic y-axis) for the same topology. Nodes with solar-recharged batteries operate under varying PSFs and channel failures over a 10-year simulation with a real weather dataset (Section 3.2).

Across the above conditions, the distributions of RBEs are closely aligned due to consistent trends in ECR, despite variations in solar irradiance. The RBEs range from 2618.57 mAh to 15 000 mAh, the full battery capacity. These consistency results demonstrate RNTP's energy management efficiency, ensuring reliable performance under diverse conditions.

These results stem from RNTP's transport control mechanisms (Section 2.4.2), which dynamically select efficient subpaths and reduce unnecessary transmissions (Section 2.4.1). The mechanisms reduce the energy impact of interference and congestion, ensuring reliable and efficient operation.

3.5 Comparative Studies

Statistics. Figs. 11(a), 11(b), and 11(c) demonstrate that RNTP consistently keeps significantly lower EEFRs, EEDTs, and EECs. Its comparative schemes include RNTP, TCP-AODV, UDP-AODV, TCP-DSR, UDP-DSR, TCP-DSDV, UDP-DSDV, DAF, RT-CaCC, and FRP. RNTP achieves notable statistics for NNs (5, 10, 15) under 30 dB mean noise:

- Mean EEFRs of (0, 0.02, 0.02)%
- Mean EEDT-Ns of (0.8, 1.75, 2.75) s.
- Mean EEDT-Rs of (1.52, 3.62, 5.54) s.
- Mean EECs of (0.18, 0.19, 0.19) J.

In contrast, other schemes exhibit notably higher mean EEFRs, EEDTs, and EECs. For NN at 15 under 30 dB mean noise, their performance is characterized as follows:

- Mean EEFRs of 38.77%, 27.31%, 32.68%, 22.58%, 40.59%, 42.02%, 24.88%, 74.87%, and 54.45%.
- Mean EEDTs of 24.01 s, 16.41 s, 28.78 s, 13.91 s, 26.26 s, 25.22 s, 14.94 s, 44.96 s, and 32.67 s.
- Mean EECs of 0.29, 0.25, 0.27, 0.23, 0.46, 0.47, 0.24, 0.72, and 0.4 J.

These statistics witness RNTP's performance superiority.

Explanation. The superior performance of RNTP is attributed to fundamental differences in scheme designs.

The first is route establishment. TCP or UDP-based protocols (AODV, DSR, and DSDV) and NDN-based protocols (DAF and RT-CaCC) establish routes solely by hop count, often selecting unreliable paths with a low SINR or the received signal strength indication (RSSI) [14], increasing packet losses. In contrast, FRP uses a low RSSI threshold for constructing primary paths and in-path backup subpaths, relying on per-hop message flooding. This construction results in severe packet losses due to channel contention and interference, leading to frequent establishment failures. Moreover, the in-path creation method limits the backup subpath's ability to select alternative subpaths, thereby reducing rerouting options.

The second lies in impacts of transport control policies:

- TCP's congestion control is sensitive to packet losses, often causing a halt in payload packet transmission.
- UDP sends packets aggressively, causing packet losses.
- DAF retrieves each Data packet by having the consumer send or resend an Interest packet along an unexpired end-to-end path. This one-at-a-time retrieval method is inefficient, and reliance on unreliable paths leads to worse performance, especially under high noise conditions.
- RT-CaCC lacks effective reroute and hop-by-hop congestion control, limiting its reliability for per-hop and receiver-side retransmissions in lossy environments.
- FRP lacks effective transport control.

By fully addressing these factors mentioned, our proposed RNTP stands out as an exceptional solution. It introduces SINR-based subpath route management and tightly integrates it with hop-by-hop congestion control and fast retransmission.

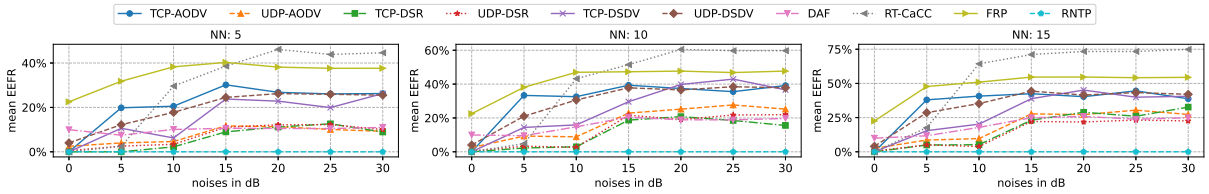

(a) EEFR

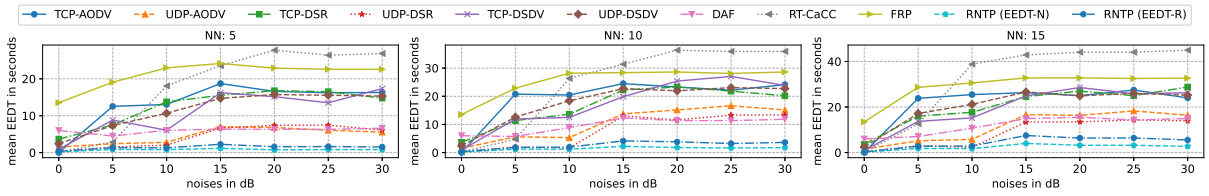

(b) EEDT

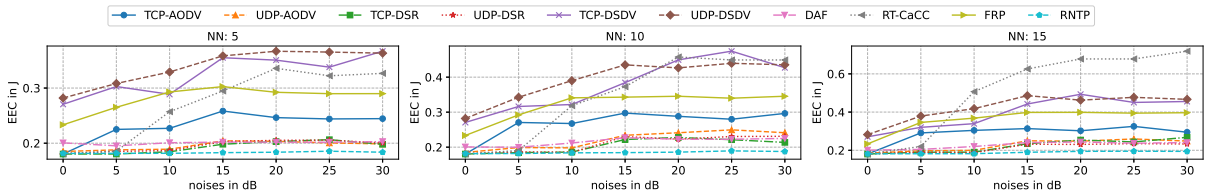

(c) EEC

Figure 11: Performance comparison of RNTP under various levels of noise interference for different NNs in the 64-node WSN

4 Conclusion

The proposed RNTP is a robust subpath-based NDN transport protocol that enhances resiliency over existing schemes. By utilizing efficient per-hop control and a novel subpath routing structure, RNTP optimizes node trajectories and enhances rerouting options. It employs a low-complexity one-pass flooding approach for subpath route establishment and selects high-metric subpaths based on SINR and hop count for balanced payload forwarding. Congestion control and fast retransmissions are achieved through an optimized AIMD policy, significantly improving overall resiliency.

Through comprehensive simulations in stationary ad-hoc WSNs, RNTP outperforms existing protocols, showing lower EEFR, EEDT-N, EEDT-R, and EEC. It also maintains efficient message exchanges and scales well with network size, achieving superior energy efficiency and stable performance under adverse conditions. These results demonstrate RNTP's suitability for energy-constrained applications in outdoor WSNs.

We suggest further research in integrating RNTP with existing Internet of Things (IoT) platforms, extending it to mobile ad-hoc WSNs, and adapting it for real-world sensor data monitoring applications.

References

[1] M. A. Jamshed, K. Ali, Q. H. Abbasi, M. A. Imran, and M. Ur-Rehman, "Challenges, applications, and future of wireless sensors in Internet of things: A review," *IEEE Sensors Journal*, vol. 22, no. 6, pp. 5482–5494, 2022.

[2] F. Wang and J. Liu, "Networked wireless sensor data collection: Issues, challenges, and approaches," *IEEE Communications Surveys & Tutorials*, vol. 13, no. 4, pp. 673–687, 2011.

[3] M. A. Mahmood, W. K. Seah, and I. Welch, "Reliability in wireless sensor networks: A survey and challenges ahead," *Computer Networks*, vol. 79, pp. 166–187, 2015.

[4] D. K. Sah and T. Amgoth, "Renewable energy harvesting schemes in wireless sensor networks: A survey," *Information Fusion*, vol. 63, pp. 223–247, 2020.

[5] *Ad hoc On-Demand Distance Vector (AODV) Routing*, IETF Std. IETF 3561, 2003.

[6] *The Dynamic Source Routing Protocol (DSR) for Mobile Ad Hoc Networks for IPv4*, IETF Std. IETF 4728, 2007.

[7] S. Riaz, M. Rehan, T. Umer, M. K. Afzal, W. Rehan, E. U. Munir, and T. Iqbal, "FRP: A novel fast rerouting protocol with multi-link-failure recovery for mission-critical WSN," *Future Generation Computer Systems*, vol. 89, pp. 148–165, 2018.

[8] M. I. Alipio and N. M. C. Tiglao, "RT-CaCC: A reliable transport with cache-aware congestion control protocol in wireless sensor networks," *IEEE Transactions on Wireless Communications*, vol. 17, no. 7, pp. 4607–4619, 2018.

[9] D. N. M. Hoang, J. M. Rhee, and S. Y. Park, "Fault-tolerant ad hoc on-demand routing protocol for mobile ad hoc networks," *IEEE Access*, vol. 10, pp. 111 337–111 350, 2022.

[10] S. Mahajan, R. Harikrishnan, and K. Kotecha, "Adaptive routing in wireless mesh networks using hybrid reinforcement learning algorithm," *IEEE Access*, vol. 10, pp. 107 961–107 979, 2022.

[11] L. Zhang, A. Afanasyev, J. Burke *et al.*, "Named data networking," *ACM SIGCOMM Computer Communications Review*, vol. 44, no. 3, pp. 66–73, 2014.

[12] M. A. Rahman and B. Zhang, "On data-centric forwarding in mobile ad-hoc networks: Baseline design and simulation analysis," in *IEEE ICCCN*, 2021, pp. 1–9.

[13] F. Ansari, R. A. Rehman, and A. Arsalan, "Reduced network forwarding with controller enabled named software defined Internet of mobile things," *Ad Hoc Networks*, vol. 149, p. 103235, 2023.

[14] A. Goldsmith, *Wireless Communications*. Cambridge University Press, 2005.

[15] S. Mastorakis, A. Afanasyev, and L. Zhang, "On the evolution of ndnSIM: an open-source simulator for NDN experimentation," *ACM SIGCOMM Computer Communications Review*, vol. 47, no. 3, pp. 19–33, 2017.

[16] A. Tariq, R. A. Rehman, and B.-S. Kim, "Forwarding strategies in NDN-based wireless networks: A survey," *IEEE Communications Surveys & Tutorials*, vol. 22, no. 1, pp. 68–95, 2020.

[17] (2024) NDN packet format specification. [Online]. Available: https://named-data.net/doc/NDN-packet-spec/current/

[18] (2024) Resilient subpath-based NDN transport protocol. [Online]. Available: https://github.com/zhouby-zjl/rntp

[19] *IEEE Standard for Telecommunications and Information Exchange Between Systems - LAN/MAN Specific Requirements - Part 11: Wireless Medium Access Control (MAC) and physical layer (PHY) specifications: High Speed Physical Layer in the 5 GHz band*, IEEE Std. Std 802.11a, 1999.

[20] J. Seybold, *Introduction to RF Propagation*. John Wiley & Sons, 2005.

[21] S. Chaudhary, Ratigar, A. K. Mishra, and R. K. Singh, "Rate adaptation algorithms in IEEE 802.11 wireless networks: A comparative study," *Journal of The Institution of Engineers (India): Series B*, vol. 104, no. 6, pp. 1369–1375, 2023.

[22] *Transmission Control Protocol (TCP)*, IETF Std. RFC 9293, 2022.

[23] *User Datagram Protocol*, IETF Std. RFC 768, 1980.

[24] C. E. Perkins and P. Bhagwat, "Highly dynamic destination-sequenced distance vector (DSDV) for mobile computers," *ACM SIGCOMM Computer Communication Review*, 1994.

[25] A. R. Jensen, K. S. Anderson, W. F. Holmgren, M. A. Mikofski, C. W. Hansen, L. J. Boeman, and R. Loonen, "pvlib iotools—open-source python functions for seamless access to solar irradiance data," *Solar Energy*, vol. 266, p. 112092, 2023.

[26] (1999) Siemens solar module ST40. [Online]. Available: https://www.siemen.co.uk/st40.pdf

[27] (2025) Libelium devices. [Online]. Available: https://www.libelium.com/

[28] (2025) Tektelic devices. [Online]. Available: https://tektelic.com/

[29] J. A. Kratochvil, W. E. Boyson, and D. L. King, "Photovoltaic array performance model," Sandia National Laboratories, Tech. Rep., 2004. [Online]. Available: https://www.osti.gov/biblio/919131

[30] "A new solar radiation database for estimating PV performance in Europe and Africa," *Solar Energy*, vol. 86, no. 6, pp. 1803–1815, 2012.

Table 2: Summary on performance of RNTP under various levels of noise interference for different NNs in the 64-node WSN

(NN, noise in dB)		**(0, 0)**	**(5, 10)**	**(5, 20)**	**(5, 30)**	**(10, 10)**	**(10, 20)**	**(10, 30)**	**(15, 10)**	**(15, 20)**	**(15, 30)**
mean	EEFR	0%	0%	0.0%	0.0%	0%	0.02%	0.02%	0%	0.04%	0.02%
	EEDT-N	0.19 s	0.81 s	0.75 s	0.8 s	1.23 s	1.78 s	1.75 s	1.75 s	3.23 s	2.75 s
	OOR	31.34%	34.19%	32.91%	32.98%	36.02%	35.45%	35.31%	38.49%	37.62%	37.28%
	EEDT-R	0.34 s	1.29 s	1.59 s	1.52 s	1.94 s	3.81 s	3.62 s	2.9 s	6.39 s	5.54 s
	min arrival timeout	1 s	2.25 s	1.58 s	1.73 s	3.37 s	2.66 s	2.79 s	4.28 s	4.47 s	4.24 s
	Capsule queue size	26.46 p	27.19 p	31.03 p	29.82 p	28.34 p	36.63 p	37.56 p	31.66 p	38.28 p	37.61 p
95-p	EEFR	0%	0%	0%	0%	0%	0%	0%	0%	0.5%	0%
	EEDT-N	0.54 s	4.74 s	4.74 s	4.41 s	6.26 s	9.87 s	9.91 s	7.07 s	14.43 s	13.05 s
	OOR	31.34%	42.79%	41.82%	42.29%	43.78%	43.78%	44.22%	44.78%	45.27%	44.78%
	EEDT-R	0.83 s	6.69 s	10.51 s	9.81 s	8.3 s	19.03 s	17.76 s	9.76 s	25.43 s	23.09 s
	min arrival timeout	1 s	7 s	5 s	5.25 s	8 s	10.2 s	10.1 s	9	12 s	13 s
	Capsule queue size	91 p	88 p	94 p	93 p	88 p	99 p	99 p	86 p	98 p	98 p
total	msg. send rate (pps)	2.16	3.2	3.01	3.15	3.7	4.75	4.4	4.99	6.5	5.98
	msg. recv. rate (pps)	25.49	31.4	29.31	29.65	34.25	37.21	36.11	40.71	45.56	42.69
	CapAck ratio	43.26%	37.02%	36.3%	35.41%	35.65%	29.28%	31.31%	33.51%	30.53%	30.35%